Pathology - Research and Practice 215 (2019) 983–987

Contents lists available at ScienceDirect

Pathology - Research and Practice

journal homepage: www.elsevier.com/locate/prp

Sinonasal glomangiopericytoma: A clinicopathologic study

Farres Obeidin, Lawrence J. Jennings, Borislav A. Alexiev*

Department of Pathology, Northwestern University Feinberg School of Medicine, Northwestern Memorial Hospital, 251 East Huron St, Feinberg 7-342A, Chicago, IL, 60611, United States

ARTICLE INFO

Keywords:
Sinonasal glomangiopericytoma
β-catenin
TLE1
CTNNB1

ABSTRACT

Sinonasal glomangiopericytoma (SNGP) is a neoplasm arising in the nasal cavity and paranasal sinuses that shows perivascular myoid differentiation. The diagnosis of SNGP may be diagnostically challenging due to a large number of potential mimics. In the present study, we sought to characterize the histological and molecular features of six cases of SNGP found in prior surgical pathology records over a 15-year period. The average age at diagnosis was 48.5 years (range: 31–78 years), and the male-to-female ratio was 1:1. Imaging studies in all six cases demonstrated avidly enhancing, lobulated soft tissue masses in the nasal cavity, extending into the sinuses and nasopharynx. Histologically, the tumors were unencapsulated and composed of a proliferation of closely packed, bland, and uniform spindle cells growing deep to an intact surface respiratory epithelium. The cells were separated by a distinctive vascular network ranging from capillaries to large vascular spaces. All cases demonstrated strong positivity for smooth muscle actin, cyclin D1, CD99, and β-catenin (100%). Targeted sequencing revealed recurrent *CTNNB1* missense mutations in all cases tested. Additionally, TLE1 was positive in all cases which has not been previously reported. No tested cases harbored *SS18* translocations. We found that while no single marker resolves immunohistochemical overlap between SNGP and its histologic mimics, an extended immunohistochemical panel that includes β-catenin, cyclin D1, STAT6, smooth muscle actin, pancytokeratin cocktails, S100, and SOX10 helps to support the diagnosis of SNGP in diagnostically challenging cases without the need for molecular studies.

1. Introduction

Sinonasal glomangiopericytoma/sinonasal hemangiopericytoma-like tumor (SNGP) is defined by the World Health Organization (WHO) as a sinonasal mesenchymal neoplasm demonstrating a perivascular myoid phenotype. Initially described as a variant of hemangiopericytoma due to the presence of characteristic staghorn vasculature seen in other soft tissue hemangiopericytomas, immunohistochemical studies have suggested a perivascular myoid phenotype necessitating a shift in the nomenclature [1,3–5,10,11,13,14,18–20,26,28,32,33]. They occur most commonly in adults in the sixth and seventh decades of life, show a slight female predominance, and clinically mimic allergic polyps of the sinonasal tract [33]. The nasal cavity, and, less frequently, sinuses are affected. Most patients present with nasal obstruction, epistaxis, and other nonspecific findings that are present for an average of less than 1 year. A rare case of SNGP associated with severe osteogenic osteomalacia has previously been reported [20]. The diagnosis of SNGP may be diagnostically challenging in small biopsies due to the large number of potential histological mimics that may occur in this location [13]. While the molecular pathogenesis has not been completely elucidated, *CTNNB1* gene mutations and nuclear expression of β-catenin have recently been identified in SNGP [11,13,19]. A definitive diagnosis is often helpful for treatment planning, as both benign and malignant neoplasms fall within the differential for this lesion.

This study aims to: 1) evaluate the morphological features of SNGP and establish an efficient diagnostic immunohistochemical panel to distinguish it from its mimics, and 2) evaluate SNGP for recurrent genetic mutations by Sanger sequencing.

2. Material and methods

2.1. Histology

A single institution SNGP cohort of six resected tumors was identified within the last 15 years at Northwestern Memorial Hospital. Clinical, surgical, and pathologic details were obtained from the electronic medical records and the AP laboratory information system. The original pathology material was reviewed, and the tumors were

* Corresponding author at: Department of Pathology, Northwestern University Feinberg School of Medicine, Northwestern Memorial Hospital, 251 East Huron St, Feinberg 7-342A, Chicago, IL, 60611, United States.
E-mail address: Borislav.Alexiev@northwestern.edu (B.A. Alexiev).

https://doi.org/10.1016/j.prp.2019.02.004
Received 18 December 2018; Received in revised form 31 January 2019; Accepted 1 February 2019
0344-0338/

Table 1
Case demographics.

Case	Age	Sex	Clinical presentation	Location	Size	Follow-up	Outcome
1	40	M	Epistaxis	Right nasal septum	2.1 cm	8 months	Alive; NED
2	46	M	Nasal obstruction	Right nasal cavity; nasopharynx, ethmoid sinus	5.5 cm	10 years	Alive; LR
3	78	F	Epistaxis	Left posterior ethmoid and sphenoid sinuses	1.5 cm	8 years	Alive; NED
4	51	M	Incidental finding	Left nasal cavity	1.5 cm	9 years	Alive; NED
5	31	F	Proptosis	Right inferior orbit	2.0 cm	4 years	Alive; LR
6	59	F	Nasal obstruction and epistaxis	Bilateral nasal cavity and left ethmoid sinus	1.6 cm	2 months	Alive; NED

NED: No evidence of disease; LR: Local recurrence.

classified based on current criteria [33]. Representative/extensive tissue sections from the surgical specimens were fixed in 10% buffered formalin and embedded in paraffin. For routine microscopy, 4-μm-thick sections were stained with hematoxylin-eosin.

2.2. Immunohistochemistry

Immunohistochemical staining was performed using an automated immunostainer (Leica Bond-III, Leica Biosystems, Buffalo Grove, IL) and Bond Refine PolymerTM biotin-free DAB detection kit. A panel of immunohistochemical stains was performed and included: cytokeratin AE1/AE3 (Dako; M3515; 1:500; Santa Clara, CA), desmin (Leica; PA0032; RTU; Buffalo Grove, IL), CD34 (Leica; PA0212; RTU; Buffalo Grove, IL), S100 (Leica; PA0900; RTU; Buffalo Grove, IL), SOX10 (Abcam; ab227684; 1:80; Cambridge, MA), STAT6 (Abcam; ab32520; 1:1000; Cambridge, MA), smooth muscle actin (Leica; PA0943; RTU; Buffalo Grove, IL), cyclin D1 (Epitomics; AC-0017; 1:100; Burlingame, CA), CD99 (Dako; M3601; 1:100; Santa Clara, CA), β-catenin (Dako; M3539; 1:100; Santa Clara, CA), and TLE1 (Abcam; ab183742; 1:200; Cambridge, MA). Nuclear, cytoplasmic, and/or membranous expression identified in 10% or more of neoplastic cells was defined as "positive." Positive immunostains were then categorized as "focal positive (F+)" if expression was 10–24% of neoplastic cells, and "diffuse positive (+)" if expression was ≥25%. Formalin-fixed, paraffin-embedded (FFPE) tissue from five solitary fibrous tumors was used as a control for immunoprofile comparison with SNGP.

2.3. Targeted sequencing

The use of paraffin blocks for this study meets Institutional Review Board and Health Insurance Portability and Accountability Act requirements, and has been approved by the Institutional Review Board at the Northwestern University Feinberg School of Medicine. Hematoxylin-eosin stained slides were chosen from the same blocks reviewed by a pathologist. No microdissection was needed, as all samples had > 50% tumor cells per section. Due to the small size of a few cases, two of six cases were depleted by immunostains and could not be sequenced for *CTNNB1* or analysed for *SS18-SSX* translocation.

For each case, DNA was extracted from a single 5 μm section according to the manufacturer's instructions (Covaris truXTRAC FFPE DNA kit (Woburn, MA, USA)). Briefly, slides were warmed on a heat block to 37 °C for 30 s and FFPE tissue was then scraped from the slides, avoiding paraffin, using Covaris sectionPICKs. Sections were collected into screw-cap microtubes by using FFPE sectionPICKs provided by Covaris. Sonication was performed per the manufacturer's instructions on a Covaris M220 Focused Ultrasonicator. Homogenized tissue was then digested for 2 h in Covaris proteinase K at 56 °C. DNA was finally isolated from lysates using the columns of the Covaris truXTRAC FFPE DNA kit and was eluted in 100 μL of Covaris BE buffer.

The DNA concentration and quality was assessed using a Nanodrop spectrophotometer by NanoDrop Technologies (Life Technologies) as per manufacturer's instructions. Targeted Sanger sequencing was used to identify mutations of *CTNNB1*, exon 3. After PCR amplification of the targeted exon, 10 μL of amplicon was transferred to a new PCR tube and 1 μL of ExoSAP-IT® (Affimetrix, Santa Clara, CA) was added to remove unused dNTPs and primers per manufacturer's instructions. The sequencing reaction was performed using 2 μL of the cleaned product and the "Big Dye Terminator v1.1 Cycle Sequencing" kit (Life Technologies, Carlsbad, CA) by the M13 forward primer 5′ - TGT AAA ACG ACG GCC AGT - 3′ and reverse primer 5′ - CAG GAA ACA GCT ATG ACC - 3′, in an ABI Prism 3130 xl automatic sequencer (Life Technologies, Carlsbad, CA) in both directions. Data were analysed by Sequencing Analysis (Life Technologies, Carlsbad, CA).

For each case, RNA was extracted from a single 5 μm section according to the manufactuer's instructions (Covaris truXTRAC FFPE DNA kit (Woburn, MA, USA)). The extracted RNA was converted to cDNA using the SuperScript VILO cDNA Synthesis Kit from Invitrogen (Life Technologies, Grand Island, NY) following the manufacturer's instructions. Synovial sarcoma fusion transcripts were targeted (SS18-SSX1, SS18-SSX2, SS18-SSX4, SS18-SSX7, and SS18-SSX8) using 2 different primer pairs. A SYBR Green qPCR assay was preformed using the Bio-Rad iQ5 Real-Time Detection System and amplified to the end-point. Thermal cycling conditions were 37oC x 30 min (1 cycle), 95oC x 10 min (1 cycle), 95oC x 30 s and 60oC x 30 s (2 cycles), 95oC x 30 s and 68oC x 30 s (38 cycles), followed by a melt curve which ranged from 55oC-95oC at 0.5oC increments, and 12oC hold. The analysis of the qPCR data was performed with the iQ5 Optical System Software from Bio-Rad, which generates cycle threshold (Ct) values and melt curve plots. The quality of RNA was verified by amplification of a longer transcript corresponding to the ubiquitously expressed GUSB.

3. Results

3.1. Clinical history

The case demographics are listed in Table 1. Six cases were found in prior surgical pathology records at Northwestern Memorial Hospital from 2003 to 2018 using the search terms "sinonasal hemangiopericytoma" and "sinonasal glomangiopericytoma." All patients were treated at Northwestern Memorial Hospital with endoscopic sinus surgery alone. There were equal numbers of males and females. The median age was 48.5 years old (range 31–78 years), and the median follow-up time was 6 years (range 2 months-10 years). All patients were alive at the most recent follow-up.

3.2. Imaging studies and gross description

Computed tomography scans and magnetic resonance imaging demonstrated avidly enhancing, lobulated soft tissue masses in the nasal cavity, extending into the sinuses and nasopharynx, abutting the undersurface of the anterior skull base (Fig. 1). Grossly, SNGPs presented as polypoid, pink-tan or red-brown soft tissue fragments with homogenous cut surfaces and areas of hemorrhage. Tumor size ranged from 1.5 to 5.5 cm with a mean of 2.6 cm.

3.3. Histology

Histologically, the tumors were unencapsulated and composed of a

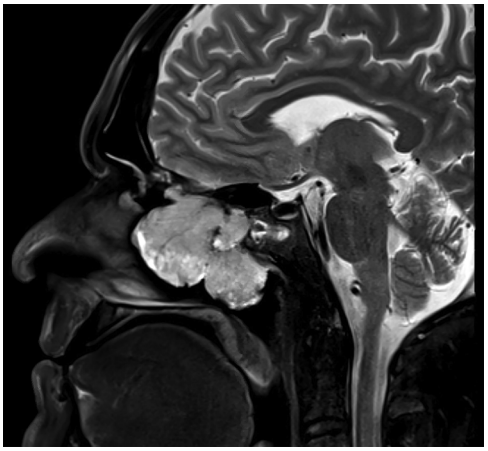

Fig. 1. Sinonasal glomangiopericytoma. Magnetic resonance imaging demonstrated avidly enhancing, lobulated soft tissue masses in the nasal cavity.

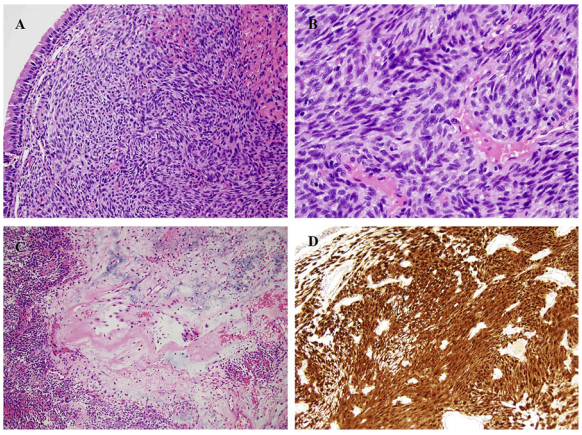

Fig. 2. Sinonasal glomangiopericytoma. A. Note the proliferation of closely packed, bland, uniform, spindled cells with a fascicular to focally whorled architecture underlying an intact surface respiratory epithelium. B. Tumor cells are oval to spindle-shaped with hyperchromatic nuclei, inconspicuous nucleoli, and limited eosinophilic cytoplasm. C. Some areas show myxoid change and prominent perivascular hyalinization. D. Strong nuclear β-catenin expression in tumor cells, original magnification ×200 (A); ×400 (B); ×100 (C); ×200 (D).

subepithelial proliferation of closely packed, bland, and uniform spindle cells deep to an intact surface respiratory epithelium. SNGPs showed a diffuse growth with fascicular to solid or focally whorled patterns (Fig. 2A). The nuclei were ovoid to spindled, varying from vesicular to hyperchromatic with inconspicuous nucleoli and limited eosinophilic cytoplasm (Fig. 2B). The cells were separated by a distinctive vascular network ranging from capillaries to large vascular spaces. Prominent acellular and perivascular hyalinization was often present (Fig. 2C). Myxoid change, areas of fibrosis, and interstitial mast cells and eosinophils were commonly observed. Mitotic figures were inconspicuous, and necrosis absent.

3.4. Immunohistochemistry

All cases of SNGP demonstrated nuclear β-catenin, SMA, CD99, cyclin D1, and TLE1 immunostaining in ≥50% of the tumor cells (6/6, 100%) (Figs. 2D and 3 A–C). CD34 was focally positive with weak to moderate cytoplasmic intensity in five of six tumors (83%). All SNGPs failed to demonstrate cytokeratin AE1/AE3, STAT6, desmin, S100, and SOX10 positivity (Fig. 3D), (Table 2).

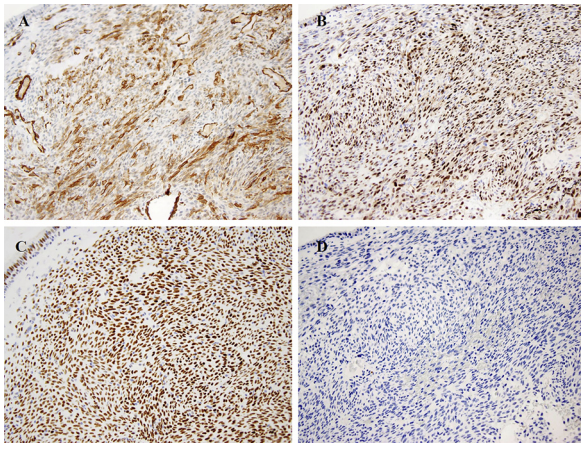

Fig. 3. Sinonasal glomangiopericytoma. A. Smooth muscle actin expression in tumor cells. B. Cyclin D1 expression in tumor cells. C. TLE1 expression in tumor cells. D. Tumor cells are negative for STAT6. Bond Refine PolymerTM biotin-free DAB detection kit, original magnification ×200 (A–D).

Table 2
Sinonasal glomangiopericytoma. Immunohistochemical findings.

Case	1	2	3	4	5	6
SMA	+	+	+	+	+	+
β-catenin	+	+	+	+	F+	+
CD34	+	F+	F+	F+	–	F+
CD99	+	+	+	+	+	+
Cyclin D1	+	+	+	+	+	F+
TLE1	+	+	+	+	+	+
Desmin	–	–	–	–	–	–
AE1/AE3	–	–	–	–	–	–
SOX10	–	–	–	–	–	–
S100	–	–	–	–	–	–
STAT6	–	–	–	–	–	–

–(negative, < 10%); F+ (focal positive, 10–25%); + (diffuse positive, > 25%).

3.5. Targeted sequencing

Cases 1–3 and 6 had enough tissue available for additional *CTNNB1* testing. All 4 cases that had tissue available for sequencing showed missense mutations involving the recognition site of the β-catenin destruction complex (NM_001098209.1:c.98C > T:p.S33 F, c.110C > T:p.S37 F, c.110C > T:p.S37 F, and c.134C > T:p.S45 F). In all cases, a serine residue was mutated, preventing the phosphorylation and proteasomal degradation of the β-catenin protein (Fig. 4). The mutant protein was therefore stabilized, leading to accumulation in the nucleus and increased transcription of Wingless-related integration

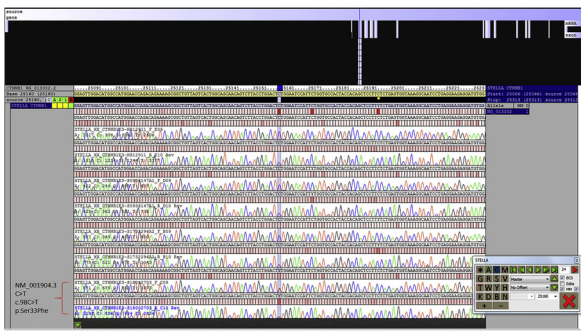

Fig. 4. Sinonasal glomangiopericytoma. A. Representative electropherogram showing all molecular aberrations in *CTNNB1* seen. All cases showed point mutations in serine residues leading to inhibition of phosphorylation and degradation of β-catenin.

site target genes (i.e. Wnt signaling pathway). Mutations of these 3 residues have recently been associated with SNGP and proposed as a key oncogenic driver [19].

3.6. Synovial sarcoma fusion analysis

Due to the scant tissue remaining after IHC and *CTNNB1* analysis, only cases 1, 2, and 6 could be assessed for synovial sarcoma fusions. All 3 cases were negative for *SS18-SSX1*, *SS18-SSX2*, *SS18-SSX4*, *SS18-SSX7*, and *SS18-SSX8*.

4. Discussion

SNGP is a neoplasm demonstrating perivascular myoid differentiation that arises in the nasal cavity and paranasal sinuses [18]. SNGP comprises < 0.5% of all sinonasal neoplasms. In the present study, six cases were found by searching through prior surgical pathology records over a 15-year period. The average age at diagnosis was 48.5 years, and the male-to-female ratio was 1:1. The diagnosis of SNGP may be diagnostically challenging due to the large number of potential mimics with varying degrees of histological and immunohistochemical overlap [4,13].

Hemangiopericytoma (HPC) was described in 1942 by Stout and Murray as a distinctive soft tissue neoplasm presumably of pericytic origin, which exhibited a characteristic well-developed "staghorn" branching vascular pattern [10]. Three categories of lesions are now thought to exist within the heterogeneous group of HPC-like neoplasms. The first category corresponds to those neoplasms that show clear evidence of myoid/pericytic differentiation and correspond to true HPCs. They include myopericytoma, infantile myofibromatosis (previously called infantile HPC), and SNGP. The second category is the solitary fibrous tumor (SFT) lesional group, which includes fibrous-to-cellular SFTs and related lesions such as giant cell angiofibromas. The third category corresponds to those non-HPC neoplasms that occasionally display HPC-like features, including synovial sarcoma (SS) and malignant peripheral nerve sheath tumor [10].

Histologically, SNGP demonstrates a number of features that differ from SFT. The cytologically uniform tumor cells often appear to be placed equidistant from one another, and there is at least focal fascicular growth. This contrasts with the patternless SFT architecture, characterized by a combination of hypocellular and hypercellular areas separated by thick bands of hyalinized collagen [9,10,12]. The small round capillaries and ectatic blood vessels within the tumor nodules of SNGP also differ from the multibranched staghorn vessels seen in SFT [9,10,12]. In agreement with previous studies, we found that SNGP showed convincing evidence of perivascular myoid differentiation, strong nuclear β-catenin, cyclin D1, SMA, and CD99, and harbored *CTNNB1* missense mutations in the amino-terminal region [1,3–5,10,11,13,14,18–20,16,28,33]. SNGPs lack nuclear STAT6 expression and *NAB2-STAT* translocations, in contrast to their presence in sinonasal SFTs [1,9,10,12,31].

Myopericytoma is a benign neoplasm demonstrating perivascular myoid differentiation that may be confused with SNGP. Architecturally, myopericytomas are well-circumscribed with a nodular or lobular growth pattern and uniform spindled or ovoid cells showing frequent perivascular concentric growth around HPC-like vessels [13]. The tumor shows variable cellularity and can have collagenous or myxoid stroma. Owing to their similar cell of origin, smooth muscle actin expression is shared between both myopericytoma and SNGP. Consistent genetic alterations have not been identified in myopericytoma, apart from a unique variant characterized by translocation t(7;12)(p22;q13) which results in *ACTB–GLI1* fusion and a report of *BRAF* V600E mutation in a subset of myopericytomas [13]. Nuclear β-catenin expression is consistently absent and is useful in the distinction between these tumors [13].

Biphenotypic sinonasal sarcoma (BSNS) is a rare recently-described low grade malignant mesenchymal neoplasm with neural and myogenic differentiation seen exclusively in the upper sinonasal tract. BSNS shows histological and immunohistochemical overlaps with a number of lesions at this site [8,15,21,29]. BSNS is characterized by infiltrating spindle-shaped cells with minimal pleomorphism, low mitotic activity, and concomitant benign epithelial proliferation. The neoplasm exhibits immunopositivity for both SMA and S-100 [8,15,21,29]. β-catenin immunoreactivity is seen in the majority of cases, indicating a role in pathogenesis. A distinguishing characteristic of BSNS is that it displays a dual neural and myogenic phenotype, with variable immunopositivity for S-100, along with SMA, calponin, desmin, and even focal myogenin positivity [15]. BSNS is characterized by recurrent genetic alterations involving *PAX3* gene, with *MAML3* being the most frequent fusion partner [15].

A critical differential to consider in cases of suspected SNGP is spindle cell (monophasic) SS, due to its malignant behavior and potential for adjuvant therapy. Monophasic SS is characterized by uniform spindle cells arranged in cellular sheets and fascicles. Tumor cells have overlapping, ovoid nuclei with pale eosinophilic cytoplasm and indistinct cells borders. Many monophasic SSs focally display a staghorn-shaped vascular pattern, reminiscent of SFT/HPC, and myxoid change. Classically, SS shows at least focal positivity for epithelial markers such as cytokeratins and EMA, as well as CD99. SMA and HHF-35 are typically not expressed [2,6,27,30]. Similar to SNGP, frequent β-catenin expression in SS was observed in previous studies [13,32]. However, nuclear β-catenin correlates with cyclin D1 expression in SNGP but not in SS [30]. Though TLE1 was initially thought to be relatively specific for SS, recent studies have shown strong TLE1 expression in nerve sheath tumors and SFT [7,17]. Additionally, strong positivity for TLE1 was seen in all six of our cases of SNGP, so this marker clearly cannot be relied upon to resolve this differential. SS is characterized by translocation t(X;18)(p11;q11), resulting in *SS18* gene rearrangement with one of three *SSX* gene fusion partners (*SSX1*, *SSX2*, or *SSX4*) [2,6,27,30]. This translocation was not seen in any of our tested cases.

Low grade myofibroblastic sarcoma (LGMS) may also be considered in the differential for tumors of the nasal cavity and paranasal sinus, since it appears to have a strong predilection for the head and neck region in younger patients. LGMS is characterized by aggressive local behavior with low potential for metastasis. Histologically, the tumor shows a diffusely infiltrative growth pattern and consists mainly of spindle cells with minimal pleomorphism, low mitotic activity, and abundant pale eosinophilic cytoplasm. Immunohistochemically, LGMS are positive for vimentin, fibronectin, and at least one muscle marker, including alpha-smooth muscle actin, HHF-35, calponin, or desmin [23,24]. Nuclear β-catenin expression is consistently absent in LGMS.

Intranasal glomus tumor and SNGP are both characterized by a perivascular growth pattern and share immunohistochemical features supporting their myoid differentiation by expression of muscle specific markers [16,22,25]. A novel gene fusion involving *MIR143* with *NOTCH-1*, *NOTCH-2*, or *NOTCH-3* has been recently identified in benign and malignant glomus tumors [25]. The *MIR143-NOTCH* fusions were not identified in SNGP. Conversely, glomus tumors do not harbor *CTNNB1* missense mutations and are negative for nuclear β-catenin. These results argue that glomus tumors are genetically distinct from most myopericytic tumors and SNGP, despite their perivascular growth patterns and shared immunophenotype [25].

SNGP is an indolent tumor that tends to arise in the sinonasal tract of older adults and has a low malignant potential with excellent prognosis after surgical resection [4,32,33]. Surgery was the treatment of choice for all six of our patients, and none received adjuvant therapy. All six patients are alive, and four of them are free of disease. Two patients showed continued disease at their last follow-up. Recurrent tumors were managed by additional surgery.

Our results in this study demonstrate that mutational activation of β-catenin and associated cyclin D1 overexpression may be central to the pathogenesis of SNGP. However, due to the positivity of these markers

in other tumors, including SFT, BSNS, and SS, their roles are limited among this differential list if used alone. Similarly, TLE1 cannot be used to exclude SS, as all of our cases stained positively for TLE1. The considerable overlap in the morphological features and immunohistochemical expression of various markers between these entities poses diagnostic difficulties to pathologists in small biopsies [13]. In the majority of cases, the diagnosis of SNGP can be facilitated by recognition of its diffuse proliferation of uniform spindle and ovoid cell population, hemangiopericytoma-like vessels, nuclear β-catenin expression, and perivascular myoid phenotype. While no single marker resolves immunohistochemical overlap between SNGP and its histologic mimics, an extended immunohistochemical panel that includes β-catenin, cyclin D1, STAT6, smooth muscle and/or muscle specific actin, broad-spectrum cytokeratin cocktails (AE1/AE3, CAM5.2), S100, and SOX10 helps to support the diagnosis of SNGP in diagnostically challenging cases without the need for molecular studies.

Conflict of interest

None of the authors have any conflict of interest to disclose.

Funding sources

None.

Disclaimer

All authors have seen and approved the manuscript, and contributed significantly to the work. The manuscript has not been previously published, nor is it being considered for publication elsewhere.

References

[1] A. Agaimy, S. Barthelmeß, H. Geddert, C. Boltze, E.A. Moskalev, M. Koch, S. Wiemann, A. Hartmann, F. Haller, Phenotypical and molecular distinctness of sinonasal haemangiopericytoma compared to solitary fibrous tumour of the sinonasal tract, Histopathology 65 (2014) 667–673.
[2] J.J. Barrott, B.E. Illum, H. Jin, J.F. Zhu, T. Mosbruger, M.J. Monument, K. Smith-Fry, M.G. Cable, Y. Wang, A.H. Grossmann, M.R. Capecchi, K.B. Jones, β-catenin stabilization enhances SS18-SSX2-driven synovial sarcomagenesis and blocks the mesenchymal to epithelial transition, Oncotarget 6 (2015) 22758–22766.
[3] M. Brandwein-Gensler, G.P. Siegal, Striking pathology gold: a singular experience with daily reverberations: sinonasal hemangiopericytoma (glomangiopericytoma) and oncogenic osteomalacia, Head Neck Pathol. 6 (2012) 64–74.
[4] M. Dandekar, J.B. McHugh, Sinonasal glomangiopericytoma: case report with emphasis on the differential diagnosis, Arch. Pathol. Lab. Med. 134 (2010) 1444–1449.
[5] A.K. El-Naggar, J.G. Batsakis, G.M. Garcia, M.L. Luna, H. Goepfert, Sinonasal hemangiopericytomas. A clinicopathologic and DNA content study, Arch. Otolaryngol. Head Neck Surg. 118 (1992) 134–137.
[6] S.S. Fatima, N.U. Din, Z. Ahmad, Primary synovial sarcoma of the pharynx: a series of five cases and literature review, Head Neck Pathol. 9 (2015) 458–462.
[7] W.C. Foo, M.W. Cruise, M.R. Wick, J.L. Hornick, Immunohistochemical staining for TLE1 distinguishes synovial sarcoma from histologic mimics, Am. J. Clin. Pathol. 135 (2011) 839–844.
[8] K.J. Fritchie, L. Jin, X. Wang, R.P. Graham, M.S. Torbenson, J.E. Lewis, M. Rivera, J.J. Garcia, D.J. Schembri-Wismayer, J.J. Westendorf, M.M. Chou, J. Dong, A.M. Oliveira, Fusion gene profile of biphenotypic sinonasal sarcoma: an analysis of 44 cases, Histopathology 69 (2016) 930–936.
[9] I. Ganly, S.G. Patel, H.E. Stambuk, M. Coleman, R. Ghossein, D. Carlson, M. Edgar, J.P. Shah, Solitary fibrous tumors of the head and neck: a clinicopathologic and radiologic review, Arch. Otolaryngol. Head Neck Surg. 132 (2006) 517–525.
[10] C. Gengler, L. Guillou, Solitary fibrous tumour and haemangiopericytoma: evolution of a concept, Histopathology 48 (2006) 63–74.
[11] F. Haller, M. Bieg, E.A. Moskalev, S. Barthelmeß, H. Geddert, C. Boltze, N. Diessl, K. Braumandl, B. Brors, H. Iro, A. Hartmann, S. Wiemann, A. Agaimy, Recurrent mutations within the amino-terminal region of beta-catenin are probable key molecular driver events in sinonasal hemangiopericytoma, Am. J. Pathol. 185 (2015) 563–571.
[12] Y. Han, Q. Zhang, X. Yu, X. Han, H. Wang, Y. Xu, X. Qiu, F. Jin, Immunohistochemical detection of STAT6, CD34, CD99 and BCL-2 for diagnosing solitary fibrous tumors/hemangiopericytomas, Int. J. Clin. Exp. Pathol. 8 (2015) 3166–3175.
[13] V.Y. Jo, C.D.M. Fletcher, Nuclear β-catenin expression is frequent in sinonasal hemangiopericytoma and its mimics, Head Neck Pathol. 11 (2017) 119–123.
[14] E.S. Jung, S.W. Yang, J.H. Kim, S.W. Kim, A case of glomangiopericytoma involving the orbital wall, Ear Nose Throat J. 92 (2013) E13–5.
[15] A. Kakkar, M. Rajeshwari, P. Sakthivel, M.C. Sharma, S.C. Sharma, Biphenotypic sinonasal sarcoma: A series of six cases with evaluation of role of β-catenin immunohistochemistry in differential diagnosis, Ann. Diagn. Pathol. 33 (2018) 6–10.
[16] J. Kim, J. Jeon, D.H. Kim, E.S. Park, L.S. Maeng, S.Y. Jun, Glomangiopericytoma and glomus tumor of the sinonasal tract: A report of two cases with emphasis on the differential diagnosis, Pathol. Int. 66 (2016) 348–350.
[17] K. Kosemehmetoglu, J.A. Vrana, A.L. Folpe, TLE1 expression is not specific for synovial sarcoma: a whole section study of 163 soft tissue and bone neoplasms, Mod. Pathol. 22 (2009) 872–878.
[18] F.Y. Kuo, H.C. Lin, H.L. Eng, C.C. Huang, Sinonasal hemangiopericytoma-like tumor with true pericytic myoid differentiation: a clinicopathologic and immunohistochemical study of five cases, Head Neck 27 (2005) 124–129.
[19] J. Lasota, A. Felisiak-Golabek, F.Z. Aly, Z.F. Wang, L.D. Thompson, M. Miettinen, Nuclear expression and gain-of-function β-catenin mutation in glomangiopericytoma (sinonasal-type hemangiopericytoma): insight into pathogenesis and a diagnostic marker, Mod. Pathol. 28 (2015) 715–720.
[20] G.G. Lee, H.J. Dhong, Y.S. Park, Y.H. Ko, Sinonasal glomangiopericytoma causing oncogenic osteomalacia, Clin. Exp. Otorhinolaryngol. 7 (2014) 145–148.
[21] J.T. Lewis, A.M. Oliveira, A.G. Nascimento, D. Schembri-Wismayer, E.A. Moore, K.D. Olsen, J.G. Garcia, M.L. Lonzo, J.E. Lewis, Low-grade sinonasal sarcoma with neural and myogenic features: a clinicopathologic analysis of 28 cases, Am. J. Surg. Pathol. 36 (2012) 517–525.
[22] X.Q. Li, M. Hisaoka, T. Morio, H. Hashimoto, Intranasal pericytic tumors (glomus tumor and sinonasal hemangiopericytoma-like tumor): report of two cases with review of the literature, Pathol. Int. 53 (2003) 303–308.
[23] G.Z. Meng, H.Y. Zhang, H. Bu, G.H. Yang, X.L. Zhang, G. Yang, Myofibroblastic sarcoma of the nasal cavity and paranasal sinus: a clinicopathologic study of 6 cases and review of the literature, Oral Surg. Oral Med. Oral Pathol. Oral Radiol. Endod. 104 (2007) 530–539.
[24] T. Mentzel, S. Dry, D. Katenkamp, C. Fletcher, Low-grade myofibroblastic sarcoma: analysis of 18 cases in the spectrum of myofibroblastic tumors, Am. J. Surg. Pathol. 22 (1998) 1228–1238.
[25] J.M. Mosquera, A. Sboner, L. Zhang, C.L. Chen, Y.S. Sung, H.W. Chen, N.P. Agaram, D. Briskin, B.M. Basha, S. Singer, M.A. Rubin, T. Tuschl, C.R. Antonescu, Novel MIR143-NOTCH fusions in benign and malignant glomus tumors, Genes Chromosom. Cancer 52 (2013) 1075–1087.
[26] J.C. Oosthuizen, S. Kennedy, C. Timon, Glomangiopericytoma (sinonasal-type haemangiopericytoma), J. Laryngol. Otol. 126 (2012) 1069–1072.
[27] A.A. Owosho, C.L. Estilo, E.B. Rosen, S.K. Yom, J.M. Huryn, C.R. Antonescu, A clinicopathologic study on SS18 fusion positive head and neck synovial sarcomas, Oral Oncol. 66 (2017) 46–51.
[28] E.S. Park, J. Kim, S.Y. Jun, Characteristics and prognosis of glomangiopericytomas: A systematic review, Head Neck 39 (2017) 1897–1909.
[29] L.M. Rooper, S.C. Huang, C.R. Antonescu, W.H. Westra, J.A. Bishop, Biphenotypic sinonasal sarcoma: an expanded immunoprofile including consistent nuclear β-catenin positivity and absence of SOX10 expression, Hum. Pathol. 55 (2016) 44–50.
[30] T. Saito, Y. Oda, H. Yamamoto, K. Kawaguchi, K. Tanaka, S. Matsuda, Y. Iwamoto, M. Tsuneyoshi, Nuclear beta-catenin correlates with cyclin D1 expression in spindle and pleomorphic sarcomas but not in synovial sarcoma, Hum. Pathol. 37 (2006) 689–697.
[31] S.C. Smith, W.E. Gooding, M. Elkins, R.M. Patel, P.W. Harms, A.S. McDaniel, N. Palanisamy, C. Uram-Tuculescu, B.B. Balzer, D.R. Lucas, R.R. Seethala, J.B. McHugh, Solitary fibrous tumors of the head and neck: a multi-institutional clinicopathologic study, Am. J. Surg. Pathol. 41 (2017) 1642–1656.
[32] L.D. Thompson, M. Miettinen, B.M. Wenig, Sinonasal-type hemangiopericytoma: a clinicopathologic and immunophenotypic analysis of 104 cases showing perivascular myoid differentiation, Am. J. Surg. Pathol. 27 (2003) 737–749.
[33] L.D.R. Thomson, U. Flucke, B.M. Wenig, Sinonasal glomangiopericytoma, in: A.K. El-Naggar, J.K.C. Chan, J.R. Grandis, T. Takata, P.J. Slootweg (Eds.), WHO Classification of Head and Neck Tumours, 4th ed., IARC Press, Lyon, 2017, pp. 44–45.